Provided for non-commercial research and education use.
Not for reproduction, distribution or commercial use.

This article appeared in a journal published by Elsevier. The attached copy is furnished to the author for internal non-commercial research and education use, including for instruction at the authors institution and sharing with colleagues.

Other uses, including reproduction and distribution, or selling or licensing copies, or posting to personal, institutional or third party websites are prohibited.

In most cases authors are permitted to post their version of the article (e.g. in Word or Tex form) to their personal website or institutional repository. Authors requiring further information regarding Elsevier's archiving and manuscript policies are encouraged to visit:

http://www.elsevier.com/copyright

Author's personal copy

Journal of Theoretical Biology 265 (2010) 151–159

Contents lists available at ScienceDirect

Journal of Theoretical Biology

journal homepage: www.elsevier.com/locate/yjtbi

Predicting the buoyancy, equilibrium and potential swimming ability of giraffes by computational analysis

Donald M. Henderson [a,*], Darren Naish [b]

[a] Royal Tyrrell Museum of Palaeontology, PO Box 7500, Drumheller, AB, Canada T0J 0Y0
[b] School of Earth and Environmental Sciences, University of Portsmouth, Portsmouth, UK

ARTICLE INFO

Article history:
Received 2 September 2009
Received in revised form
4 April 2010
Accepted 5 April 2010
Available online 10 April 2010

Keywords:
Flotation
Locomotion
Scaling
Three-dimensional digital models

ABSTRACT

Giraffes (*Giraffa camelopardalis*) are often stated to be unable to swim, and while few observations supporting this have ever been offered, we sought to test the hypothesis that giraffes exhibited a body shape or density unsuited for locomotion in water. We assessed the floating capability of giraffes by simulating their buoyancy with a three-dimensional mathematical/computational model. A similar model of a horse (*Equus caballus*) was used as a control, and its floating behaviour replicates the observed orientations of immersed horses. The floating giraffe model has its neck sub-horizontal, and the animal would struggle to keep its head clear of the water surface. Using an isometrically scaled-down giraffe model with a total mass equal to that of the horse, the giraffe's proportionally larger limbs have much higher rotational inertias than do those of horses, and their wetted surface areas are 13.5% greater relative to that of the horse, thus making rapid swimming motions more strenuous. The mean density of the giraffe model (960 gm/l) is also higher than that of the horse (930 gm/l), and closer to that causing negative buoyancy (1000 gm/l). A swimming giraffe – forced into a posture where the neck is sub-horizontal and with a thorax that is pulled downwards by the large fore limbs – would not be able to move the neck and limbs synchronously as giraffes do when moving on land, possibly further hampering the animal's ability to move its limbs effectively underwater. We found that a full-sized, adult giraffe will become buoyant in water deeper than 2.8 m. While it is not impossible for giraffes to swim, we speculate that they would perform poorly compared to other mammals and are hence likely to avoid swimming if possible.

Crown Copyright © 2010 Published by Elsevier Ltd. All rights reserved.

1. Introduction

The singular shape of the giraffe *Giraffa camelopardalis* has invited many questions about its biology, ecology and evolution. It remains controversial as to how many cervical vertebrae giraffes have (Solounias, 1999), and debate continues as to whether their necks evolved for sexual selection (Simmons and Scheepers, 1996) or not (Mitchell et al., 2009), or to provide a competitive advantage over contemporary herbivores (Cameron and du Toit, 2007). The giraffe's long limbs and neck, sloping back and short body give it a distinctive gait (Powell, 1984).

Terrestrial locomotion in giraffes has been little studied, and even less is known about the behaviour of giraffes in water. It is generally thought that giraffes cannot swim, but relevant observations are few. Shortridge (1934) and Goodwin (1954) state that giraffes were poor waders and unable to swim. Crandall (1964) discussed a case where a captive giraffe escaped from a carrying crate, ran to the end of a jetty, and fell into the water. The animal reportedly sank without making any attempt to swim. MacClintock (1973, p. 54) stated 'Giraffes cannot swim. Rivers are barriers they do not cross'. Wood (1982, p. 20) noted that 'Because of its extraordinarily anatomical shape the giraffe is one of the very few mammals that cannot swim – even in an emergency! Deep rivers are an impassable barrier to them, and they will avoid large expanses of water like the plague'.

While these claims and observations may have merit, scepticism is required about assertions that certain animals cannot swim (e.g., camels and pigs swim well, despite claims to the contrary; Shortridge, 1934). Furthermore, the idea that giraffes are poor waders or will not cross rivers is incorrect (Kingdon, 1989), and there do not seem to be obvious reasons why giraffes might be more prone to sinking than other mammals. The bone density of giraffes is similar to that of other big mammals, although giraffe limb bones are slightly thicker that those of bovids (van Schalkwyk et al., 2004).

In view of the history of claims about the inability of giraffes to swim, and inspired by previous studies on the floating and swimming behaviour of other tetrapods (Henderson 2003a, b, 2006), we became interested in testing the hypothesis that giraffes perform poorly in water. If their poor performance in

* Corresponding author. Tel.: +01 403 820 6218; fax: +01 403 823 7131.
E-mail address: don.henderson@gov.ab.ca (D.M. Henderson).

0022-5193/$ - see front matter Crown Copyright © 2010 Published by Elsevier Ltd. All rights reserved.
doi:10.1016/j.jtbi.2010.04.007

Author's personal copy

water results from their unusual body shape, this should become evident from experiments devised to test the buoyancy and equilibrium (and not necessarily the swimming ability) of a giraffe in water. For practical and ethical reasons we are unable to use live giraffes, and instead explored this hypothesis using digital models whose component masses can be compared quantitatively and software that simulates flotation (Henderson, 2003a, b, 2006). Given all the uncertainties and non-linear effects associated with the hydrodynamics of moving tetrapod limbs and bodies in water, we chose to focus on static properties of the limbs and bodies to make our assessment of potential swimming ability.

2. Methods

2.1. Model generation

Horse body and limb shapes (Fig. 1a) were taken from Simpson (1951, Plate I) in combination with observations of live horses (DMH), while those of the giraffe (Fig. 1b) were based on the illustrations showing multiple views presented in Kingdon (1989). The horse illustrated in Simpson was not identified to breed, and although not critical to the present study, the slender trunk, limbs and head suggest that it is a thoroughbred. The model forms of each animal were collected using digital slicing (Henderson, 1999). This involves sampling both limbs and the axial body using closely spaced lines that cross both dorsal and ventral, or left and right, profiles at selected points with variable separation between the lines. The points of intersection between cross-cutting lines and body outlines are used to define the sets of semi-minor and semi-major diameters of the body or body part. These diameters, and the separations between them, are used to define the model as a series of contiguous, irregular slabs of elliptical cross-section. The ears for the two models, as well as the ossicones and the solid part of the giraffe's tail, were produced using the same technique. The tail of the horse, composed of a multitude of fine, low-mass hairs, was not modeled. For presentation of the flotation states, both models of Fig. 1 had the number of body and limb defining slabs increased by a factor of four, and the number of polygons per slab increased from 16 to 128. In anticipation of their orientations when floating, the heads of the floated models were rotated upwards by 20–30° relative to that in a normal standing posture. This resulted in the eyes and nose being above, or close to, the water line. Additionally, as the limbs of the floated models were no longer bearing the weight of the body and being maintained in an erect fashion, they were flexed slightly to emphasise their relaxed condition. The basic giraffe model was also enhanced by applying a synthetic giraffe blotch pattern (Appendix A). For both models the coordinate axes were set up as follows: the XY-plane corresponds to the sagittal plane with the *X*-axis parallel to the ground (or water surface) with increasing values towards the head, and the *Y*-axis vertical and at right angles to the *X*-axis; *Z*-axis is perpendicular to the sagittal plane with positive values corresponding to the right side of the body.

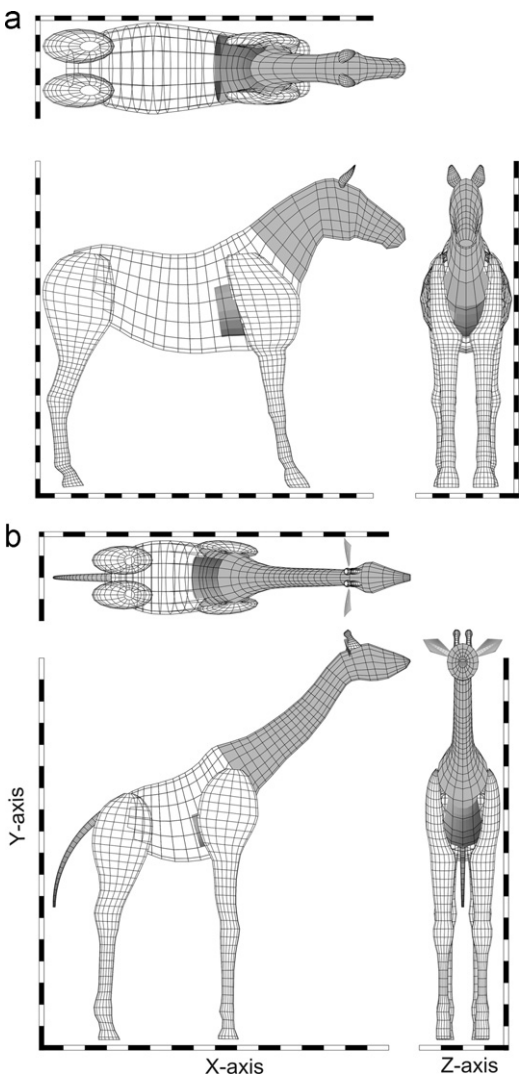

Fig. 1. Isometric views of the three-dimensional computational models used in this study. (a) Horse (*Equus caballus*) with scale bar increments of 10 cm. (b) Giraffe (*Giraffa camelopardalis*) with scale bar increments of 25 cm. The light grey colouring of the heads and necks highlight the lower density of 850 gm/l used for this portion of the body, when compared to the 1000 gm/l for the remainder of the axial body and the 1050 gm/l for the limbs. The dark grey cylinder in the thoracic region represents the estimated lung volume. See Methods for more detail on density estimates and lung volumes, and Table 1 for summary data on each model.

2.2. Body mass and centre of mass determinations

Estimates for the masses and centres of mass of the models are key components for flotation modeling. The downward weight force (a product of mass and gravitational acceleration) causes the model to displace water as it is pulled down, and the upward buoyant force acting on the model is proportional to the volume of water displaced. The final equilibrium state of the model is set when the downwards weight is balanced by the upwards buoyant force. The centre of mass (CM) of the complete model is the point about which the model will rotate when subject to torques arising from the buoyant forces (Henderson, 2003a). The masses of the limbs are used to determine the final mass of the model, and in combination with their CMs, the CM of the body+limb system. As the shoulder girdles of most mammals move with the fore limb (Hildebrand, 1982), the fore limb mass of both models includes the mass of the tissues enclosing the scapula. Additionally, the positions and distances of the limb CMs relative to the CM of the axial body are important for determining whole body rotational inertias (RIs) (see below). Finally, as the limbs hang passively during the flotation simulations, the limbs are set to hang with their CMs directly beneath their associated shoulder or hip sockets.

The contiguous set of elliptical slabs used to define the body and limb shapes also facilitated determination of the model masses. The mass of a slab is the product of its volume and its density, and assigning particular densities to sets of slabs from different body regions allows for a more finely resolved, and

Author's personal copy

accurate, representation of the mass distribution within the models. The densities of the heads and necks of the giraffe and horse models (light grey regions in Fig. 1) were set at 850 gm/l in consideration of the sinuses in the head, the oral and nasal cavities, and the oesophagus and trachea, while the post-cervical region was initially set to 1000 gm/l (see below for details regarding lung volume and associated thoracic density). The limbs, with their higher proportions of dense bone and muscle (van Schalkwyk et al., 2004), had their densities set uniformly to 1050 gm/l (Taylor, 1993). Full details of the mathematical methods for these mass and CM calculations can be found in Henderson (1999, 2003a).

2.3. Lung volume determination

The size, shape and position of the modeled lungs exerts an important effect on each model's final depth of immersion and orientation ("trim"; Henderson, 2003a). A lung volume for the horse was computed using the scaling relationship established for mammals by Stahl (1967):

$$V_{\text{lung}} = 53.5\, M_{\text{body}}^{1.06} \tag{1}$$

where lung volume, V_{lung}, is in millilitres and body mass, M_{body}, is in kilograms. Use of Eq. (1) is complicated slightly by the fact that M_{body} already includes the effect of the mass reduction associated with the cavity represented by the lungs. Actual application of Eq. (1) to determine a lung volume involved an iterative process that started with an estimated initial lung volume and converged towards a final answer. This iterative process can be expressed as:

$$V_{\text{lung}}^{1} = 53.5 \cdot \left(M_{\text{body}} - \frac{V_{\text{lung}}^{0}}{1000} \right)^{1.06} \tag{2}$$

where V_{lung}^{0} is the initial lung volume estimate, and V_{lung}^{1} is the improved estimate, and this process is repeated by substituting the most recent value of V_{lung}^{1} as a new value for V_{lung}^{0} until the desired level of precision is attained. The division of V_{lung}^{0} by 1000 inside the parentheses of Eq. (2) simultaneously converts this initial volume quantity (measured in millilitres) to litres. With the initial assumption that the post-cervical density is the same as that of water (1000 gm/l), this litre volume automatically has a mass in kilograms. For the horse, this process resulted in a lung volume estimate of 30 l. The vital capacity of an adult horse was shown to be approximately 42 l (Couetil et al., 2000), but it is considered unlikely that a horse would ever take a breath of this volume (Robinson, 2007).

There exists some controversy about the exact lung volume in the giraffe, with estimates ranging from as low as 10 l (Patterson et al., 1957) to as high as 47 l (Robin et al., 1960). Application of the Stahl lung volume equation using the estimated giraffe model mass of 1685 kg (with no lung cavity) gave a suspiciously large value of 141 l. This equation would appear to be either unreliable at large body size, or not applicable to an unusual body form such as that of the giraffe, and a similar suggestion was made by Stahl (1967, p. 454). Harrison (1980) provided a rough rule that the giraffe lung volume was equal to eight times that of a human. With a typical adult human lungs having a maximum volume of 6 l (Chiras, 1999), this rule predicts a giraffe volume of 48 l. Assuming that the average mass of an adult giraffe is 1100 kg (Kingdon, 1989), a simple linear scaling of lung volume from this latter mass to the higher model mass results in a model lung volume of 74 l. Given the uncertainties in giraffe lung volumes, this latter value must be taken as provisional.

2.4. Flotation dynamics

Determining the flotation characteristics of a model is a multi-step process that starts with mathematically slicing the axial body and each of the limbs into 100 transverse discs of constant thickness. As the long axis of the axial body in a floating model is approximately horizontal, its transverse discs are oriented on their edges. With the limbs hanging vertically, their transverse discs are horizontal and parallel to the water surface. The degrees of immersion of each disc are computed, as are the centroids of their immersed volumes. The combined volumes of the immersed portions of the body+limb discs are used to compute the magnitude of the upwards buoyant force. The set of individual immersed volumes and their centroids for the axial body and limbs are used to compute the centre of buoyancy (CB) for the entire model. The distance between CB and CM forms the lever arm of the upwards buoyant force, and the torque formed by this lever arm and the buoyant force will cause the model to pitch forwards and backwards until an equilibrium condition is reached where there are no external torques acting on the model. As the models are bilaterally symmetric, torques acting about the longitudinal or vertical axes of the bodies were not considered. Full details of the flotation calculations and the determination of final equilibrium can be found in Henderson (2003a).

2.5. Rotation dynamics

RI is an important parameter for understanding the forces associated with the rotations and oscillations of limbs and bodies (Halliday et al., 1993). RIs of the model's axial body and limbs were determined by resampling the original meshes using equally spaced slices that were orthogonal to each element's long axis, and calculating the axial body's RI with respect to its CM, and those of the arms and legs relative to the glenoid and acetabulum, respectively. The axis of rotation in all cases was set as being perpendicular to the sagittal plane and parallel to the Z-axis. This results in RI being a measure of the axial body's resistance to pitching forward and back, and the limb's resistance to protraction and retraction. Further details of these calculations can be found in Henderson (2003a, Appendix A).

2.6. External surface area

Friction between an object's surface and a surrounding fluid can significantly retard forward motion (McMahon and Bonner, 1983). With the three-dimensional models defined as polygon meshes, it is possible to compute the magnitudes and relative proportions of the wetted surfaces of the models to see how frictional drag could potentially affect swimming ability. All the polygons defining the model surfaces are quadrilaterals defined by four vertices, and the total external area of a limb or the axial body is determined by summing the areas of all the component polygons. Each polygon is divided diagonally into two triangles, and the expression to compute the total surface area of a model, A_{surf}, is:

$$A_{\text{surf}} = \frac{1}{2} \cdot \sum_{n=0}^{P-1} \left\{ \left\| \vec{v}_0^{\,n} \times \vec{v}_1^{\,n} \right\| + \left\| \vec{v}_1^{\,n} \times \vec{v}_2^{\,n} \right\| \right\} \tag{3}$$

where $\vec{v}_0^{\,n}$, $\vec{v}_1^{\,n}$ and $\vec{v}_2^{\,n}$ are the vectors defined between, respectively, the first and second, first and third, and first and fourth perimeter points on the nth polygon, and P is the number of polygons comprising the model. The vector pair $\vec{v}_0^{\,n}$ and $\vec{v}_1^{\,n}$ define two sides of the first triangle of a quadrilateral polygon, while $\vec{v}_1^{\,n}$ and $\vec{v}_2^{\,n}$ define two sides of the second triangle.

Author's personal copy

2.7. Scaling down of the giraffe model

To make a meaningful comparison between the floating and potential swimming characteristics of the horse and giraffe it was decided to isometrically scale down the giraffe model from its full size of 1634 kg so that it would have the same mass as the horse model of 383 kg. With models of equal mass the effects of different body and limb shapes and proportions on flotation and potential swimming ability can be assessed independent of linear body size. The masses, surface areas and RIs of geometrically similar shapes of different size were expressed as mathematical functions (ratios) of their characteristic length, and these relations were used to produce a correctly scaled-down giraffe model.

For geometrically similar objects their masses will be proportional to the cubes of their characteristic lengths (Alexander, 1998). For the giraffe this length was taken to be the straight-line distance between the tip of the snout and the midpoint of the rump, and was determined for the scaled-down giraffe with the following expression:

$$\frac{M_{orig}}{L_{orig}^3} = \frac{M_{new}}{L_{new}^3} \tag{4}$$

where M_{orig} is the full body mass of the original giraffe model, L_{orig} is the full snout-rump distance, M_{new} is the required full body mass of the scaled-down form, and L_{new} is the to-be-determined characteristic length. The axial mass for the scaled-down model was also determined using Eq. (4), but with the axial mass substituted for the full body mass in M_{orig}.

The surface areas of geometrically similar objects will be proportional to the squares of their characteristic lengths (Alexander, 1998). The surface area of the scaled-down giraffe was derived from that of the full-sized model with the following expression:

$$\frac{A_{orig}}{L_{orig}^2} = \frac{A_{new}}{L_{new}^2} \tag{5}$$

where A_{orig} and A_{new} are the original and scaled-down surface areas, respectively, L_{orig} and L_{new} and are the associated characteristic lengths.

The RIs of the components of the scaled-down giraffe were computed using an expression that exploited the geometric similarity between the limbs and axial bodies of the full-sized and scaled-down models. The RI of an object can be shown to be proportional to the square of its characteristic length multiplied by its mass, and the expression for computing the RI of geometrically similar, scaled-down form is:

$$\frac{RI_{orig}}{L_{orig}^2 \cdot M_{orig}} = \frac{RI_{new}}{L_{new}^2 \cdot M_{new}} \tag{6}$$

where RI_{orig}, L_{orig} and M_{orig} are the RI, characteristic length and mass, respectively, of the full-sized form and RI_{new}, L_{new} and M_{new} are the equivalent quantities for the scaled-down form.

3. Results

Table 1 summarizes the basic features and flotation characteristics of the three models (one horse and two giraffe models), while Figs. 2 and 3 presents visual demonstrations of the final, equilibrium states of the floating horse and giraffe models. The horizontal black line in these latter two figures represents the water surface, and has a vertical (Y-axis) coordinate of 0, so immersed portions will have y-coordinates less than 0. In this section all references to the giraffe model will be to the scaled-down version. Equilibrium in this case is when buoyant forces acting to lift the models up are exactly balanced (countered) by gravity forces pulling the model down, and the buoyant torques acting on the front and back halves of the models also cancel each other to give a non-rotating model. The horse model (Fig. 2) does a reasonable job of replicating the orientation of an actual floating horse (Brado, 1984, p. 298), and provides a level of confidence in

Table 1
Parameters of computational models of a horse, a full-size giraffe and an isometrically scaled-down giraffe ($Giraffe_{SD}$).

	Horse	Giraffe	$Giraffe_{SD}$	$\frac{Giraffe_{SD}-Horse}{Horse} \times 100\%$
Mass (kg)				
Axial body[a]	254.9	913.0	219.1	−13.3
Arm	24.46	148.5	34.82	+42.4
Leg	39.64	200.6	46.94	+18.4
Total	383.1	1,611	383.0	0.0
Length (m)				
Axial body	2.085	3.971	2.449	+17.5
Arm	1.437	3.147	1.941	+35.1
Leg	1.391	2.849	1.756	+26.2
Rotational inertia[b] (kg/m^2)				
Axial body[a]	60.81	703.9	62.78	+3.24
Arm	3.600	133.2	11.88	+228
Leg	7.351	131.0	11.64	+58.3
Average density (kg/m^3)	929.5	960.0	960.0	+3.39
Lung volume (l)	30.05	74.0	18.6	−37.9
Centre of mass (floating) (x,y,z)	(0.685, −0.312, 0.0)	(0.875, −0.591, 0.0)	(0.539, −0.364, 0.0)	
Centre of Buoyancy (x,y,z)	(0.687, −0.343, 0.0)	(0.888, −0.607, 0.0)	(0.547, −0.374, 0.0)	
External surface area (m^2)				
Axial body[c]	2.956	7.159	2.723	−7.88
Arm	0.7164	2.581	0.9819	+37.1
Leg	0.8515	2.667	1.013	+19.0
Total	6.092	17.66	6.713	+10.2
Wetted external surface area (%)				
Body and limbs	84.9	87.2	87.7	3.30

[a] Includes effects of air space represented by lungs and trachea.
[b] Computed with respect to an axis perpendicular to the sagittal plane.
[c] Does not include areas of ears and ossicones.

Author's personal copy

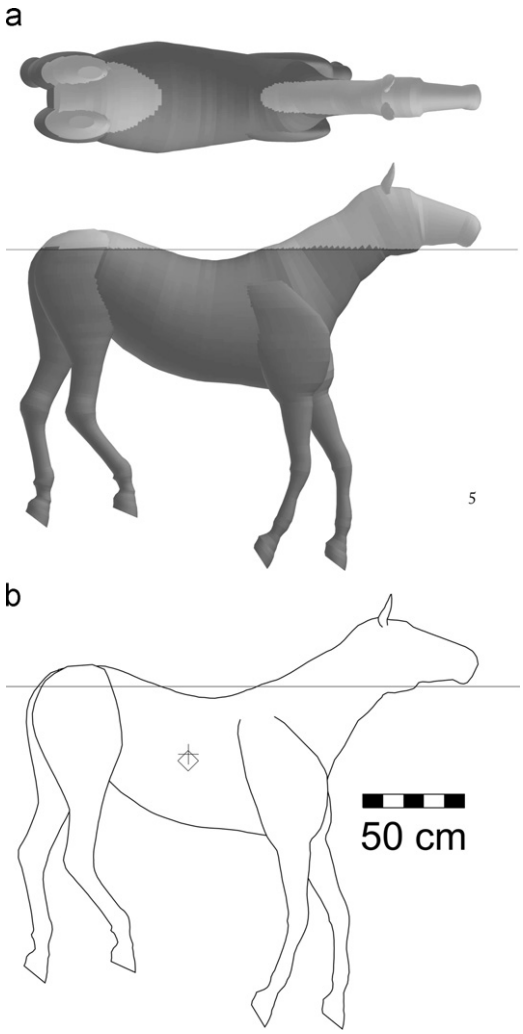

Fig. 2. Three- and two-dimensional views of the floating horse model when stable equilibrium has been attained. The black horizontal line represents the water surface and the position where the vertical (Y) coordinate is equal to zero. (a) Shaded three-dimensional model with the lighter coloured portions of the limbs and axial body indicating the "dry", exposed portions, and the thin horizontal line is the water surface. (b) Outline diagram showing the positions of the CM, '+', and the CB indicated by the diamond shape. See Table 1 for summary data on this model.

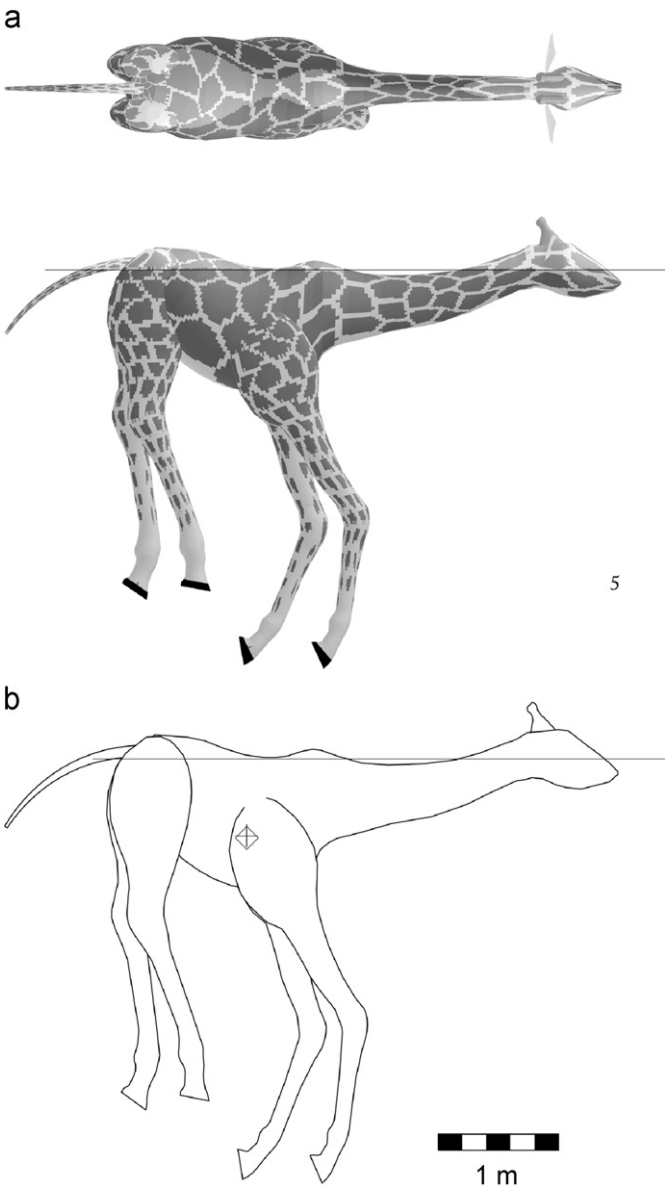

Fig. 3. Three- and two-dimensional views of the floating, scaled-down giraffe model when stable equilibrium has been attained. The relative proportions of wetted surface are almost the same for both the horse and giraffe (84.9% and 87.7%, respectively), but in absolute terms the increased surface area of the giraffe means that it has 13.5% more wetted area. See the caption for Fig. 2 for further explanation of this figure and the Appendix for generation of the blotch pattern.

the body mass distribution assigned to the model (i.e., lung volume and position, and the densities of the head, neck and limbs). This configuration of the horse is when the animal is resting *passively*. If it was actively paddling forward there would a modest upwards component of thrust that would rotate the anterior portion of the body upward, lifting the head and shoulders more, and making the dorsal surface of the back parallel to the water surface. The CB of the horse model lies about 3.1 cm below its CM.

The floating giraffe posture (Fig. 3) is similar to that of the horse in that the hips float higher than the shoulders. The giraffe body has a steeper forward inclination of 30° compared to 25° for the horse. The CB of a standing giraffe lay posterior to the CM (Fig. 5), and this had the effect of lifting the posterior portion of the body, and rotating the giraffe's neck forward and down to a sub-horizontal state. This is in contrast to the horse where the neck is only modestly rotated forwards from its terrestrial inclination (compare Fig. 1a with Fig. 2). From the study of the body mass proportions of a cull of giraffes from Zimbabwe (Mitchell et al., 2009), the mass of the head+neck of males relative to total body mass was found to be $10.8 \pm 0.4\%$. The density of the model head and neck were set to 850 gm/l, and a measure of the accuracy of this assignment is that the combined mass of the head and neck, 174.2 kg, represents 10.8% of the total body mass – a value identical to that found for the wild animals. It would appear that it is only the extensive, low-density neck that keeps the giraffe body from plunging further downwards. The head and neck of the giraffe would have also to be extended even more than what is seen in the horse to enable the animal to breathe freely and to have a clear view of its surroundings as the mouth and nostrils are fully immersed in the floating model. As in the horse the CB lies below the CM, but only by approximately 1.5 cm.

Despite the somewhat provisional nature of the model giraffe lung volume, the resulting model's relative depth of immersion is roughly similar to that of horse. Here, relative depth of

Author's personal copy

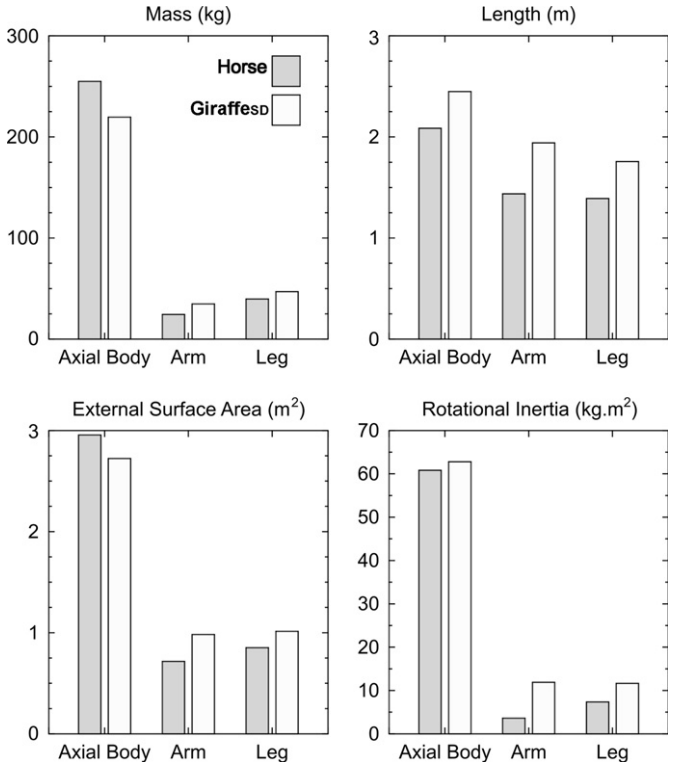

Fig. 4. Graphical depiction of the important differences between the horse and giraffe for four of the model parameters presented in Table 1. See Discussion section for the possible functional significance of these differences between the two model animals as they relate to potential swimming ability. The giraffe data is from the isometrically scaled-down model.

immersion is calculated as the percentage that the vertical depth of the CM represents of the mid-trunk depth. For the horse these latter two quantities are −0.312 and 0.60 m, and for the giraffe they are −0.591 and 1.04 m. This gives relative depths of 52% and 57% for the horse and giraffe, respectively. This suggests that the lung volume estimate is at least plausible. A further test of the influence of lung volume on buoyancy was done by repeating the flotation tests for both models, horse and giraffe, with the lungs deflated by 50%. With deflation, the mean body densities increased from their full-lung values of 929 to 967 gm/l, and from 960 to 989 gm/l in the horse and giraffe, respectively. In both cases the models remained buoyant, with each model being 7 cm more deeply immersed. The higher mean density for the giraffe, either with full or partially deflated lungs, shows that it is closer to being negatively buoyant (density > 1000 gm/l) than the horse is. The higher mean giraffe density also explains its deeper relative depth of immersion.

Fig. 4 is a graphic summary of four of the parameters presented in Table 1. The contrasting body shapes of the horse and giraffe can be seen in the differences in the relative mass proportions of the axial body and limbs for the two models. The giraffe has more of its mass in its limbs than does the horse. The mass of the giraffe arm is almost three quarters (74%) that of the leg. In contrast the horse arm mass represents 62% of its leg mass. The combination of higher limb mass and longer limbs results in much higher RIs in the giraffe limbs; this is especially the case in the fore limbs which have RIs two and a quarter times greater than those for a horse of the same body mass. The increased relative proportions of the dense limbs relative to the axial body in the giraffe also produce the higher mean density for the model. The relative proportions of the body that are immersed are not that different between the two models at 84.9% and 87.2% (wetted external surface area of Table 1), but the absolute wetted surface area is 13.8% greater in the giraffe on account of the greater overall surface area of the model. This increased absolute surface area can be attributed to the longer and more massive limbs as the external surface area of the axial body is approximately 8% less than that of the horse.

4. Discussion

Surprisingly, the CB of the horse model lies about 3.1 cm below its CM. In previous models of surface floating alligators (Henderson, 2003a), elephants (Henderson, 2003b), and sea turtles and plesiosaurs (Henderson, 2006) the CM has been below the CB, indicating a state of stable equilibrium as the model would not have a tendency to capsize. However, at the longitudinal positions of the CM and CB in the horse trunk the body depth is 60 cm, and the 2.6 cm gap represents just 5.2% of the trunk depth, and the estimated uncertainty of values derived from the modeling process is approximately 1.5% (Henderson, 2003a). As it is known that horses can remain upright while swimming, either the animals actively counter any tendency to roll laterally, or the mass distribution or shapes assigned to the model limbs and body are not quite correct. It has been observed that drowned horses tend to roll onto their sides or go "belly up", but this may be the result of the abdomen filling up with gases produced by bacterial decomposition after death, rather than any natural instability of the immersed body. The CB of the giraffe model also lies below its CM, but only by 1.6 cm, and this gap is just 1.5% of the mid-trunk depth of 1.04 m. Despite this modest reduction in the presumed tendency to roll laterally when compared with the horse, there are several other aspects of a floating giraffe that would seem to impair its ability to move in water while freely floating.

Swimming horses use a trot (McDonnell, 2003), and this is similar to the gait used on land. Giraffes tend to use a lateral sequence walk at slower speeds, and then a pacing gait before switching to a gallop when wanting to move faster (Gambaryan, 1974). The gait used by swimming horses would provide symmetric thrusts on either side of the body, and would prevent the body from experiencing any tendency to pivot about a vertical axis. This symmetric thrust gait may also explain why swimming horses can remain upright even if their CBs truly are below their CMs. There is a dearth of information on the kinematics of swimming horses (F. Fish, pers. comm. 2010), and it is non-existent for giraffes. It is unknown if giraffes would use their same lateral sequence or pacing gait while in water. It has been observed that hippos use a very different gait in water than they do on land (Coughlin and Fish, 2009). The use of the asymmetric amble by an immersed giraffe would produce unbalanced thrusts that might act to pivot the body from side to side. This would make following a preferred direction difficult for a swimming giraffe, and require increased effort to maintain a steady course. However, any tendency to pivot by the giraffe when swimming would be partly offset by the higher RI of its axial body about the vertical *Y*-axis relative to that of the horse – 62.18 kg m^2 vs. 54.12 kg m^2.

An important component of the gait of the giraffe is the synchronous motion of the neck and limbs, as the periods and amplitudes of the forward and back oscillations of the head+neck are closely linked with those of the limbs (Dagg and Foster, 1982). Their ambling/pacing walk is associated with modest neck movements, while the fast gallop is associated with large amplitude oscillations. With a floating giraffe the neck is horizontal and the orientation of the neck relative to the limbs is not the same as when the animal is on land (Fig. 3). This situation is unlike that seen with the floating horse where the relative orientations of the body and limbs with respect to one

Author's personal copy

another are closer to their terrestrial orientations. Given the coupling between head+neck oscillations and limb motions, the horizontal neck of a floating giraffe may impair effective aquatic locomotion. Additionally, without a solid substrate for the limbs to push against, the inability to get the neck and body to oscillate in a manner to which they are accustomed might further hinder effective locomotion by a floating giraffe.

Fig. 3 shows that the CM in the floating giraffe is much further from the hips than it is in the horse where the CM is more centrally positioned between the fore and hind limbs. The long lever arm associated with any thrusts coming from the giraffe's hind limbs will produce a strong turning moment on the body. The closeness of the giraffe CM to its fore limb and associated glenoid implies that any countering moments from these limbs will be much less than those of the hind limbs. In the horse, with its centrally positioned CM, the fore and hind turning moments would be expected to be more symmetric. This estimation of turning moments has, as an underlying assumption, that the muscular force and thrust applied by the hind and fore limbs of both animals will be the same.

The 13.5% increase in the wetted surface area for the giraffe relative to the horse implies that a larger frictional drag force has to be overcome by the swimming giraffe, at the cost of increased exertion and fatigue. The increase in external area is greater for the limbs than the axial body, notably for the arms (37%), and this will be critical as these parts of the body have to move rapidly to provide a propulsive thrust when swimming. As a first approximation, the drag acting on an object moving through a fluid at a high Reynolds number is proportional to the square of its velocity (McGowan, 1999), and a 4 m long giraffe attempting to swim at 1 km/h will have a high Reynolds number on the order of 8.5×10^5. In contrast, a 2 m long horse will have Reynolds number half that of the giraffe. Pressure drag becomes more important at high Reynolds numbers so the increased lengths of the giraffe's limbs and body relative to that of the horse will require a marked increase in effort to produce forward motion. An added problem is that larger animals have slower muscle contractions (Alexander, 1998), which would make it difficult to produce the higher velocity motions required underwater. While walking on land, the giraffe limbs also have gravity acting to return the limbs to the 'neutral' vertical pose, but when immersed, the buoyancy of the limbs, plus their high drag, will impede this recovery. Additional muscular activity would be required to propel the limbs both backwards and forwards in the absence of the sub-aerial gravity-assist.

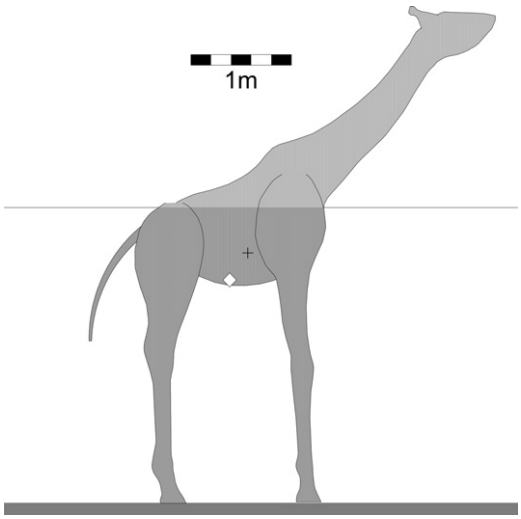

Fig. 5. Graphical demonstration of the critical water level (2.8 m) at which the upwards buoyant force and the downwards weight force are equal. Further increase in water depth will result in the model lifting off the substrate, beginning with the hind feet as the CB (white diamond) is posterior to the CM (black '+'). The CM of this standing model is slightly more posterior than that of the floating model (Fig. 3b) on account of its limbs not being swung forward.

The simultaneous increase in length and mass of the limbs also produces a substantial increase in the RI of the limbs of the giraffe relative to that of the horse – 58% more for the hind limbs and 225% for the fore limbs. Limb RI can be thought of as a proxy for the amount of effort required to either initiate or halt rotational motion of the limbs. The increase in the fore limb RI exceeds the increase in available muscle mass (Alexander, 1998), so there is a reduced capacity to change the velocity of the limbs. This may be critical when an increased rate of limb protraction and retraction is required to produce thrust while swimming.

The critical water depth for the giraffe, where the upwards buoyant force just begins to exceed the downwards weight force, was found to be 2.8 m (Fig. 5). This value was obtained by initially standing the model on 'dry' ground, and then slowly raising the simulated water level. After every increment of the water level, the buoyant forces arising from the immersed portions of the model were calculated. Fig. 5 demonstrates that an adult giraffe could potentially wade into water that was almost covering its hips, before it would start to lose contact with the substrate and begin to float, and it is reported that "they will wade quite deep rivers" (Kingdon, 1989, p. 325). However, water currents acting on the body would most likely begin to tip the model before the 2.8 m level was attained. The model predicts that at the critical water level the CB would lie behind the CM, indicating that the hind feet would leave the substrate before the fore feet would. It is unknown whether a giraffe could use just its fore limbs to punt itself along at certain water depths.

If giraffes really do avoid crossing deep bodies of water, it seems plausible that the presence of deep water channels may have had an influence on their biogeography and habitat choice. There are several indications from giraffe distribution that water has proved an obstacle to them. Spinage (1968) hypothesised that the Zambezi and its tributaries might have formed a southern barrier to the range of the Angolan and Thornicroft's giraffes and to the northern extent of the Cape giraffe's range. Goodman and Tomkinson (1987) suggested that rivers may have prevented giraffes from colonising KwaZulu-Natal and Hassanin et al. (2007) proposed that the Nile and the Great Lakes of Africa might have prevented gene flow between Kordofan and Nigerian giraffes. The Niger and Benue Rivers have also been proposed as biogeographical barriers preventing the more southerly spread of the Nigerian giraffe (Hassanin et al., 2007).

However, three considerations complicate the notion that bodies of water might have played a controlling factor in giraffe distribution. First, water bodies like the Niger River and Great Lakes are, in general, formidable zoogeographical barriers for all terrestrial mammals (Happold, 1987; Kingdon, 1990), not just for those that have poor swimming abilities. Second, the mid to late Pleistocene aridification of sub-Saharan Africa was probably the main contributor to the fragmentation of giraffe populations and hence to the resulting phylogeographic structure of extant giraffes (Brown et al., 2007). Third, because members of the genus *Giraffa* have a long history that extends back to the Miocene (and involves Eurasia as well as Africa), any effort to analyse their present distribution is complicated by prehistoric changes in climate and drainage patterns. As noted by Cramer and Mazel (2007), at least some of the areas where rivers might have formed a barrier to giraffes have been inhabited by these animals for more than 10,000 years. During such an extended period of time, major droughts and other events would have removed aquatic obstacles, and the animals would also have had enough time to find their own way around such barriers. A detailed investigation

Author's personal copy

of giraffe biogeography and its possible correlation with their poor swimming abilities is beyond the scope of this paper, however, and these comments are preliminary.

5. Conclusions

The successful replication of a floating horse by the modeling software indicates that the assumptions behind the model are plausible. The same software applied to the giraffe demonstrates that it would float, but the steep inclination of the body and sub-horizontal neck are probably not conducive to effective aquatic locomotion. The increased surface area of the giraffe in contact with the water, relative to what is observed for the horse, means that higher drag forces would have to be overcome when swimming. The longer limbs of the giraffe, with their high surface area, again in contrast to the horse, would make it more strenuous, on account of high pressure drag, for the animal to protract and retract submerged limbs at speeds suitable for aquatic propulsion. The RIs of the longer, heavier limbs of the giraffe are much greater than those of the horse, and would further impede rapid motion of the limbs for swimming. In summary, the results and speculations of this study show that it is not impossible that a giraffe could propel itself in water, but in terms of energy efficiency relative to that of the horse, it would appear that the costs of aquatic locomotion might be too high. It is reasonable to expect that giraffes would be hesitant to enter water knowing that they would be at a decided disadvantage compared to being on solid ground.

Acknowledgements

Thanks to Cameron McCormick for providing several references on the alleged inability of giraffes to swim, to E. Snively and L. Shychoski for constructive criticisms on an earlier version of the text, and to Lindie Turner for finding the Brado reference. We thank the three anonymous reviewers for their insightful reviews which made us think more carefully about what we wanted to say. DN proposed the project, DMH devised the methods, performed the analyses, and generated the figures, both DN and DMH wrote the text. DMH was supported by the Royal Tyrrell Museum and DN by the University of Portsmouth.

Appendix A. Generation of the giraffe blotch pattern

The reticulated pattern of blotches on the giraffe model was generated by a set of computational algorithms that starts with a grid of regular hexagons defined on a Cartesian grid with the horizontal *X*-axis correlated with the longitudinal axis of the body or limb, and the vertical *Y*-axis aligned with a circumferential direction around the body or limb. (Fig. A1). The sizes of a set of hexagons were chosen so that they would correspond to the sizes of blotches observed on different regions of the bodies of actual giraffes, with the hexagon set for the axial body being larger than those for the limbs. The (*X*,*Y*) coordinates of the vertices defining the hexagon grid were then displaced by a small random amounts in both the X and Y directions (Fig. A2). As adjacent hexagons share common vertices, these random vertex displacements affect neighbouring hexagons equally. Independent copies of the vertices defining each irregular hexagon (now referred to as a "blotches") were then made, and the vertices of each blotch were displaced towards their respective centres by a fixed amount. This has the effect of separating each blotch from its neighbours by a band of constant width (Fig. A3). This latter algorithm also allows for the width of the shrinkage band to be either of constant width or to vary along the length of a limb or the axial body according to a supplied function. For the limbs the spacing between the blotches increased with distance down the limb resulting in smaller blotches distally. In a real giraffe the pattern of blotches on the axial body merges seamlessly with those of the limb (Kingdon, 1989). In the model however, the limbs are generated separately from the axial body, with the result that an abrupt change in blotch size and spacing can be seen where the limbs join the body.

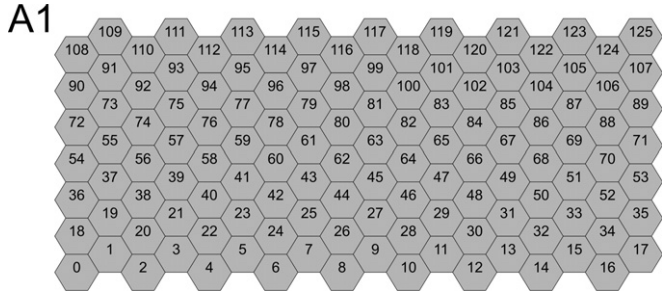

Fig. A1.

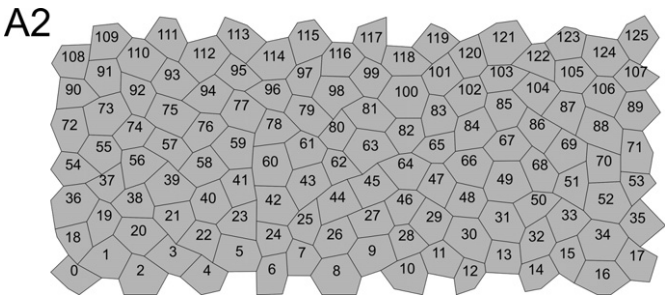

Fig. A2.

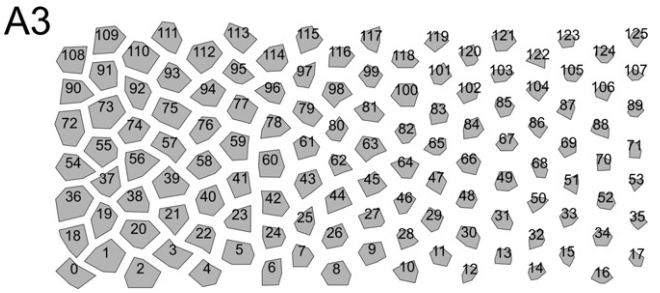

Fig. A3.

References

Alexander, R.M., 1998. All-time giants: the largest animals and their problems. Palaeontology 41, 1231–1245.
Brado, E., 1984. Early ranching in Alberta. Douglas and McIntyre, Toronto.
Brown, D.M., Brenneman, R.A., Koepfli, K.-P., Pollinger, J.P., Milá, B., Georgiadis, N.J., Louis, E.E., Grether, G.F., Jacobs, D.K., Wayne, R.K., 2007. Extensive population genetic structure in the giraffe. BMC Biology 5, 57, doi:10.1186/1741-7007-5-57.
Cameron, E.Z., du Toit, J.T., 2007. Winning by a neck: tall giraffes avoid competing with shorter browsers. The American Naturalist 169, 130–135.
Chiras, D.D., 1999. Human Biology: Health, Homeostasis, and the Environment. Jones and Bartlett Publishers, Sudbury, Massachusetts.
Couetil, L.I., Rosenthal, F.S., Simpson, C.M., 2000. Forced expiration: a test for airflow obstruction in horses. Journal of Applied Physiology 88, 1809–1870.
Coughlin, B.L., Fish, F.E., 2009. Hippopotamus underwater locomotion: reduced-gravity movements for a massive mammal. Journal of Mammalogy 90, 675–679.

Author's personal copy

Cramer, M.D., Mazel, A.D., 2007. The past distribution of giraffe in KwaZulu-Natal. South African Journal of Wildlife Research 37, 197–201.
Crandall, L.S., 1964. Management of Wild Mammals in Captivity. University of Chicago Press, Chicago, London, pp. 761.
Dagg, A.I., Foster, J.B., 1982. The Giraffe: its biology, behaviour, and ecology. Robert E. Krieger Publishing Company, Malabar, Florida.
Gambaryan, P.P., 1974. How Mammals Run. John Wiley and Sons, New York 367pp.
Goodman, P.S., Tomkinson, A.J., 1987. The past distribution of giraffe in Zululand and its implications for reserve management. South African Journal of Wildlife Research 17, 28–32.
Goodwin, G.G., 1954. In: Drimmer, F. (Ed.), The Animal Kingdom, vol. 2. Greystone Press, New York, pp. 681–874.
Halliday, D., Resnick, R., Walker, J., 1993. Fundamentals of Physics, 4th ed Wiley, New York.
Happold, D.C.D., 1987. The Mammals of Nigeria. Oxford University Press, Oxford.
Harrison, D.F.N., 1980. Biomechanics of the giraffe larynx and trachea. Acta Otolaryngologica 89, 258–264.
Hassanin, A., Ropiquet, A., Gourmand, A.-L., Chardonnet, B., Rigoulet, J., 2007. Mitochondrial DNA variability in *Giraffa camelopardalis*: consequences for taxonomy, phylogeography and conservation of giraffes in West and Central Africa. C. R. Biologies 330, 265–274.
Henderson, D.M., 1999. Estimating the masses and centers of mass of extinct animals by 3-D mathematical slicing. Paleobiology 25, 88–106.
Henderson, D.M., 2003a. Effects of stomach stones on the buoyancy and equilibrium of a floating crocodilian: a computational analysis. Canadian Journal of Zoology 81, 1346–1357.
Henderson, D.M., 2003b. Tipsy punters: sauropod dinosaur pneumaticity, buoyancy and aquatic habits. Proceedings of the Royal Society of London B (Supp.).
Henderson, D.M., 2006. Floating point: a computational study of buoyancy, equilibrium, and gastroliths in plesiosaurs. Lethaia 39, 227–244.
Hildebrand, M., 1982. Analysis of Vertebrate Structure. 2nd ed John Wiley & Sons, New York.
Kingdon, J., 1989. East African Mammals: An Atlas of Evolution in Africa, Volume III, Part B (Large Mammals). The University of Chicago Press, Chicago 60637.
Kingdon, J., 1990. Island Africa: the Evolution of Africa's Rare Animals and Plants. Collins, London.
MacClintock, D., 1973. A Natural History of Giraffes. Charles Scribner's Sons, New York, pp. 134.
McDonnell, S., 2003. A Practical Field Guide to Horse Behavior: The Equine Ethogram. The Blood-Horse Inc.
McGowan, C., 1999. A Practical Guide to Vertebrate Mechanics. Cambridge University Press, Cambridge, UK.
McMahon, T.A., Bonner, J.T., 1983. On Size and Life. Scientific American Library, New York.
Mitchell, G., van Sittert, S.J., Skinner, J.D., 2009. Sexual selection is not the origin of long necks in giraffes. Journal of Zoology 278, 281–286.
Powell, R.A., 1984. Giraffe and Okapi. In: Macdonald, D.W. (Ed.), The Encyclopedia of Mammals. Facts on File, New York, pp. 534–541.
Patterson, J.L., Warren, J.V., Doyle, J.T., Gauer, O.H., Keen, E.N., Goetz, R.H., 1957. Circulation and respiration in the giraffe. The Journal of Clinical Investigation 36, 919.
Robin, E.D., Corson, J.M., Dammin, G.J., 1960. The respiratory dead space of the giraffe. Nature 186, 24–26.
Robinson, N.E., 2007. How horses breathe: the respiratory muscles and the airways. In: McGorum, B.C., Dixon, P.M., Robinson, N.E., Schumacher, J. (Eds.), Equine Respiratory Medicine and Surgery. Saunders-Elsevier, Philadelphia, pp. 20.
Shortridge, G.C., 1934. The Mammals of South West Africa. Wm. Heinemann, Ltd., London 2 vols. 779p.
Simmons, R.E., Scheepers, L., 1996. Winning by a neck: sexual selection in the evolution of giraffe. The American Naturalist 148, 771–786.
Simpson, G.G., 1951. Horses: The Story of the Horse Family in the Modern World and Through Sixty Million Years of History. Oxford University Press, New York.
Solounias, N., 1999. The remarkable anatomy of the giraffe's neck. Journal of Zoology 247, 257–268.
Spinage, C.A., 1968. The Book of the Giraffe. Collins, London.
Stahl, W.R., 1967. Scaling of respiratory variables in mammals. Journal of Applied Physiology 22, 453–460.
Taylor, M.A., 1993. Stomach stones for feeding or buoyancy? The occurrence and function of gastroliths in marine tetrapods. Philosophical Transactions of the Royal Society of London B 341, 163–175.
van Schalkwyk, O.L., Skinner, J.D., Mitchell, G., 2004. A comparison of the bone density and morphology of giraffe (*Giraffa camelopardalis*) and buffalo (*Syncerus caffer*) skeletons. Journal of Zoology 264, 307–315.
Wood, G.L., 1982. The Guinness Book of Animal Facts and Feats. Guinness Superlatives (Enfield, Middlesex).